

A multicolor immunosensor for sensitive visual detection of breast cancer biomarker based on sensitive NADH-ascorbic acid-mediated growth of gold nanobipyramids

ZongWen Wang, Qian Chen, Yingying Zhong, Xinhui Yu, Yongning Wu, and FengFu Fu

Anal. Chem., **Just Accepted Manuscript** • DOI: 10.1021/acs.analchem.9b04828 • Publication Date (Web): 02 Dec 2019

Downloaded from pubs.acs.org on December 7, 2019

Just Accepted

“Just Accepted” manuscripts have been peer-reviewed and accepted for publication. They are posted online prior to technical editing, formatting for publication and author proofing. The American Chemical Society provides “Just Accepted” as a service to the research community to expedite the dissemination of scientific material as soon as possible after acceptance. “Just Accepted” manuscripts appear in full in PDF format accompanied by an HTML abstract. “Just Accepted” manuscripts have been fully peer reviewed, but should not be considered the official version of record. They are citable by the Digital Object Identifier (DOI®). “Just Accepted” is an optional service offered to authors. Therefore, the “Just Accepted” Web site may not include all articles that will be published in the journal. After a manuscript is technically edited and formatted, it will be removed from the “Just Accepted” Web site and published as an ASAP article. Note that technical editing may introduce minor changes to the manuscript text and/or graphics which could affect content, and all legal disclaimers and ethical guidelines that apply to the journal pertain. ACS cannot be held responsible for errors or consequences arising from the use of information contained in these “Just Accepted” manuscripts.

A multicolor immunosensor for sensitive visual detection of breast cancer biomarker based on sensitive NADH-ascorbic acid-mediated growth of gold nanobipyramids

Zongwen Wang^{†,‡}, Qian Chen[†], Yingying Zhong[†], Xinhui Yu[†], Yongning Wu[§], and FengFu Fu^{†*}

[†]Key Laboratory for Analytical Science of Food Safety and Biology of MOE, Fujian Provincial Key Lab of Analysis and Detection for Food Safety, College of Chemistry, Fuzhou University, Fuzhou, Fujian 350116, China.

[‡]State Key Laboratory of Ecological Pest Control for Fujian and Taiwan Crops, College of Plant Protection, Fujian Agriculture and Forestry University, Fuzhou 350002, China

[§]China National Center for Food Safety Risk Assessment, Beijing 100022, China.

ABSTRACT: Many studies have demonstrated that the extracellular domain of human epidermal growth factor receptor 2 (HER2 ECD) level in serum can act as a breast cancer biomarker and serve in monitoring neoadjuvant therapy of breast cancer. In this study, we developed a sensitive ascorbic acid (AA)-mediated AuNBPs (gold nanobipyramids) growth method with NADH (reduced nicotinamide adenine dinucleotide I) assistance, and further fabricated a high-resolution multicolor immunosensor for sensitive visual detection of HER2 ECD in serum by using AuNBPs as signal and antibody as recognition probe. The NADH-assisted AA-mediated method effectively suppress blank and greatly improve sensitivity of mediating AuNBPs growth, which makes us can use low concentration of AA to mediate AuNBPs growth to generate more colorful and clearer color changes. The proposed multicolor immunosensor has higher resolution and more color changes corresponding to HER2 ECD concentrations. It can be used to detect as low as 0.5 ng/mL of HER2 ECD by bare eye observation and 0.05 ng/mL of HER2 ECD by UV-visible spectrophotometry. Using the immunosensor, we have successfully detected HER2 ECD in human serum with a recovery of 94%-96% and an RSD (n=5) < 5%. The results obtained with our immunosensor were consistent with those obtained with ELISA, verifying the immunosensor has good accuracy. The immunosensor exhibited a vivid multicolor change, has low visual detection limit, excellent specificity and reproducibility, and robust resistance to matrix. All above features makes our immunosensor a promising assay for the early diagnosis of HER2-dependent breast cancers in clinical diagnosis.

Many studies have demonstrated that the patients with primary breast cancer have obvious human epidermal growth factor receptor 2 (HER2) overexpression, and thus HER2 was considered to be one of the most important prognostic and predictive factors in breast cancer.¹ HER2 protein consists of an intracellular tyrosine kinase domain, a transmembrane lipophilic segment and an extracellular domain (ECD). Undergoing proteolytic cleavage or alternative initiation of translation, the extracellular domain of HER2 protein (HER2 ECD) can be shed into the blood as a circulating antigen and be measured in serum.² Many studies have reported that the HER2 ECD levels in serum linked to tumor HER-2 overexpression,^{3,4} reflected the clinical prognosis of breast cancer,^{5,6} and thus can serve in monitoring neoadjuvant therapy in breast cancer or act as a breast cancer biomarker.⁷ Thus, the detection of HER2 ECD levels in human serum is of great clinical significance for the early diagnosis of HER2-dependent breast cancers.

So far, many analytical techniques, such as colorimetry,⁸ electrochemistry,^{9,10} fluorescence,^{11,12} and chemiluminescence,¹³ have been used for the detection of HER2 ECD. Among these techniques, the colorimetric method in particular received increasing attention because it can be read out by bare eye observation, has short detection time and low cost, and is portable. Thus, the colorimetric method has

the potential for achieving instrument-free visual on-site detection. Unfortunately, the previous colorimetric method (ELISA) for the detection of HER2 ECD only presents single color, which seriously confines the accuracy of visual inspection and thus make method has a lower sensitivity.⁸ Hence, it is of great significance to develop a high-resolution multicolor colorimetric method, which has a vivid color change, for the visual detection of HER2 ECD with high sensitivity and accuracy, in order to realize the early diagnosis and/or combination therapy of HER2-dependent breast cancers.

In recent years, gold nanocrystals (AuNCs) have been extensively applied in biological science and catalysis due to their excellent physical and chemical properties.^{14,15} One of the most interesting properties of AuNCs is localized surface plasmon resonance (LSPR), which induced strong light absorption and makes AuNCs solution showed corresponding color.¹⁶ Since the plasmon modes of AuNCs are determined by its shape, composition, size and surrounding media, a lot of colorimetric assays have been developed based on the morphology change of AuNCs via aggregation, etching or growth.¹⁷ Especially, gold nanorods (AuNRs) have two LSPR including a transverse LSPR and a longitudinal LSPR. The longitudinal LSPR of AuNRs can be regulated from 580 to 1200 nm, and thus generated a vivid color change in solution just like rainbow. Based on this phenomenon, a number of

multicolor colorimetric assays have been developed by etching or growth of AuNRs.¹⁸⁻²⁰ However, the size distributions of AuNRs produced by etching or growth usually varied in a larger range, which results in a lower intensity of color in solution and blurred color variation. Compared to AuNRs, gold nanobipyramids (AuNBPs) have obvious advantages, such as better mono-dispersity with narrow plasmon linewidths, high localized electric-field enhancements, and low-energy wavelength.²¹⁻²³ These features make ANBPs an excellent candidate for the development of multicolor colorimetric assays. For example, Xu et al developed an AuNBPs-based colorimetric immunoassay for the detection of the H5N1 virus,²⁴ and demonstrated that AuNBPs-based method has a higher sensitivity than AuNRs-based method. In this work, we developed a method of preparing high uniform AuNBPs by sensitively mediating AuNBPs growth with ascorbic acid (AA) under reduced nicotinamide adenine dinucleotide I (NADH) assistance, and further developed a high-resolution multicolor immunosensor for sensitive visual detection of HER2 ECD, in hope of providing a promising assay for the early diagnosis of HER2-dependent breast cancers in clinical diagnosis.

EXPERIMENTAL SECTION

Chemicals and Apparatus. Hexadecyl trimethyl ammonium chloride (CTAC) and citric acid were purchased from Sinopharm Chemical Reagent Co. Ltd. (Shanghai, China). Cetyltrimethylammonium bromide (CTAB), silver nitrate (AgNO_3), sodium borohydride (NaBH_4), ascorbic acid (AA) and L-ascorbic acid 2-phosphate sesquimagnesium salt (AAP) were obtained from Sigma-Aldrich Inc. (St. Louis, MO, USA). Chloroauric acid tetrahydrate ($\text{HAuCl}_4 \cdot 4\text{H}_2\text{O}$), diethanolamine (DEA), and reduced nicotinamide adenine dinucleotide I (NADH) were purchased from Aladdin Co. Ltd. (Shanghai, China). Alkaline phosphatase (ALP) was obtained from Takara Biomedical Technology Co. Ltd. (Beijing, China). Streptavidin-linked ALP was purchased from Promega Co. (Madison, WI, USA). Ab100510-HER2 ELISA Kit was purchased from Abcam Co. Ltd. (Shanghai, China). The buffer used in the experiment are as follow: PBS buffer (8 mM Na_2HPO_4 , 136 mM NaCl, 2 mM KH_2PO_4 , and 2.6 mM KCl), wash buffer (150 mM NaCl, 20 mM Tris, 0.05% Tween 20, pH 7.5). The human serums were obtained from Fujian Medical University (Fujian, China). Millipore purification system-based ultrapure water (18.2 $\text{M}\Omega \cdot \text{cm}$) was used throughout this study. The UV-visible absorption spectra were obtained with Tecan Spark 10M multifunctional microplate reader (Switzerland). All photographs were recorded by a Canon EOS 600D digital camera (Japan). Transmission electron microscope (TEM) images were performed on HT7700 transmission electron microscope (Hitachi, Japan).

Preparation of Gold Nanobipyramids Seed. The AuNBPs was synthesized by referring the typical seed-mediated method.²⁵ Firstly, 10 mL of 0.25 mM HAuCl_4 solution containing 50 mM CTAC and 5 mM citric acid was fast reduced with freshly prepared ice-cold NaBH_4 solution (0.25 mL, 25 mM) in a glass vial under vigorous stirring (1000 rpm) for 2 minutes at room temperature. Then, the obtained seed solution was statically aged for 90 min at 80°C. Finally, the obtained seed solution was kept from light at room temperature.

Colorimetric Determination of ALP. Firstly, 50 μL of different concentrations of ALP standard or sample solution, which containing 70 mM AAP, 30 mM Tris-HCl (pH 9.5), 30 mM DEA and 0.005% BSA, was prepared in a PCR tube. After incubation at 37 °C for 1 h to hydrolyze AAP to generate AA, 6.1 μL of HCl (1.0 M) was added into above solution to inhibit the activity of ALP and adjusted the pH of the solution. Then, 30 μL of above solution was taken and added into 100 μL AuNBPs growth solution, which containing 118 mM CTAB, 0.625 mM HAuCl_4 , 0.125 mM AgNO_3 , 25 mM HCl, 2 mM NADH and 1.25 μL of above AuNBPs seed solution. Finally, the whole was kept at 50 °C to perform NADH-assisted AA-mediated growth of AuNBPs for 15 min. Then, the color of the solution was observed by bare eyes and recorded by the camera, and the absorbance spectrum of solution was measured from 400-1000 nm by microplate reader. The concentration of ALP was calculated according to the color of the solution or the maximum absorption wavelength of the solution.

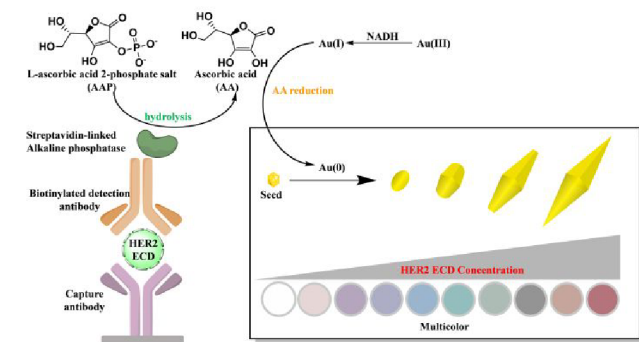
Colorimetric Determination of HER2 ECD. Firstly, 100 μL of different concentrations of HER2 ECD standard or sample solution (in PBS buffer) was added into a microplate, which previously modified with capture antibody. Then, the microplate was incubated in BE-9008 microplate oscillator for 2.5 hours at 30 °C with gentle shaking (300 rpm) to capture HER2 ECD. After washing the microplate with washing buffer (400 μL) for 4 times, 100 μL of biotinylated detection antibody (diluted 80-fold with PBS buffer) was added and the whole was incubated for 1 hour at 30 °C with gentle shaking to form "capture antibody-HER2 ECD-detection antibody" sandwich-like immunocomplex on the surface of microplate. Subsequently, 100 μL of 20 nM streptavidin-linked ALP (diluted with PBS buffer) was added and the whole was further incubated for 1 hour at 30 °C with gentle shaking. After washing the microplate with washing buffer (400 μL) for 4 times again, 50 μL of 70 mM AAP solution containing 30 mM Tris-HCl (pH 9.5), 30 mM DEA and 0.005% BSA was added and the whole was incubated at 37 °C with gentle shaking. After 1 hour, 6.1 μL of 1.0 M HCl solution and 171 μL of AuNBPs growth solution (the mixture of 118 mM CTAB, 0.625 mM HAuCl_4 , 0.125 mM AgNO_3 , 25 mM HCl, 2 mM NADH and 2.0 μL of AuNBPs seed solution) were added into the microplate and incubation at 50 °C for 20 minutes. Finally, the color of the solution was observed by bare eyes and recorded by the camera, and the absorbance spectrum of solution was measured from 400-1000 nm by Tecan Spark 10M microplate-reader. The concentration of HER2 ECD was calculated according to the color of the solution or the maximum absorption wavelength of the solution.

For the determination of human serum sample, the serum was firstly diluted 3-fold with PBS buffer and then was determined with above method.

RESULTS AND DISCUSSION

The Principle of the Strategy for Multicolor Visual Detection of ALP and HER2 ECD. In our strategy, antibody was used as probe for recognizing HER2 ECD, NADH was used to previously reduce Au (III) into Au (I) to suppress blank and improve the sensitivity of AA-mediated AuNBPs growth, and ALP was used as a readout enzyme to hydrolyze AAP to generate AA, which was used to reduce Au (I) into Au (0) and thus mediates AuNBPs growth. The detail principle of

the multicolor immunosensor for HER2 ECD detection was shown in Scheme 1. The capture antibody immobilized on the surface of microplate can specifically captured HER2 ECD and biotinylated HER2 ECD-specific detection antibody to form a “capture antibody-HER2 ECD-detection antibody” sandwich-like immunocomplex on the surface of microplate. The sandwich-like immunocomplex can quantitatively bind with streptavidin-linked ALP via biotin-avidin interaction. In the presence of AAP, the ALP can hydrolyze AAP to generate AA, and the generated AA promoted the AuNBPs growth by reducing Au (I) into Au (0) and thus generated color change. The amount of generated AA was proportional to the concentration of HER2 ECD or ALP, and with the increase of AA concentration, the morphology of grown AuNBPs changed from AuNBPs seed structure to AuNBPs structure, which accompanied with rainbow-like colors change from colorless to wine red. This provided a multicolor sensing platform for visual detection of HER2 ECD or ALP by only bare eye observation.



Scheme 1. Schematic illustration of the principle for multicolor visual detection of HER2 ECD based on NADH-assisted AA-mediated growth of Au NBPs together with antibody.

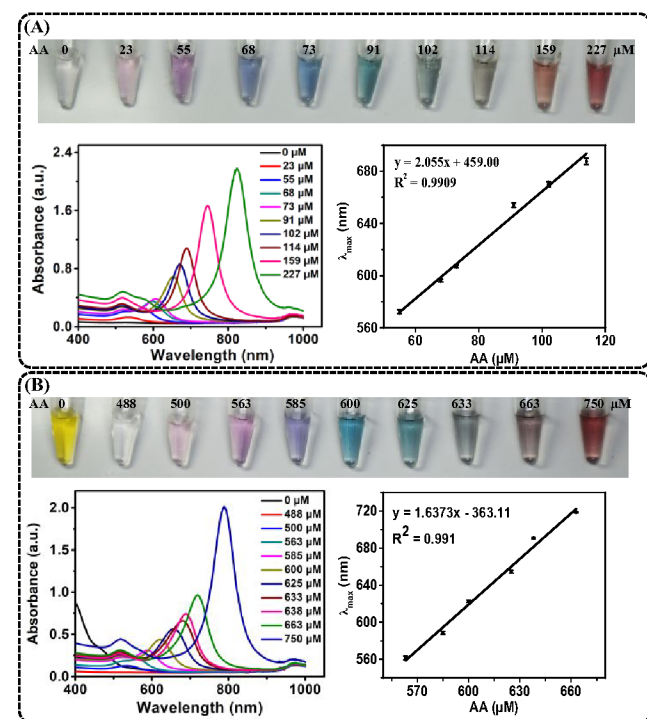


Figure 1. (A): The photographs and UV-visible spectra of AuNBPs solution obtained with NADH-assisted AA-mediated system, and their linear relationship between maximum

absorption wavelength (λ_{\max}) and AA concentration; (B): The photographs and UV-visible spectra of AuNBPs solution obtained with only AA-mediated system, and their linear relationship between λ_{\max} and AA concentration.

Sensitively Mediate the AuNBPs Growth with AA under the NADH Assistance. The sensitive regulation of AuNBPs growth and the suppression of blank are two key points in this study since Au (III) solution showed deep yellow color. In previous studies,²⁵ the AuNBPs were all prepared by directly reducing Au (III) into Au (0) with only AA. In this case, the AuNBPs-based multicolor sensors have serious blank interference and low sensitivity since Au (III) showed deep yellow color and a large part of generated AA was consumed to reduce Au (III) into Au (I) at first. As Figure 1-B showed, without NADH assistance (only AA was employed to reduce Au (III) for mediating AuNBPs growth), the system has a deep yellow blank and showed no color signal when AA concentration is lower than 500 μM , i.e. the visual detection limit of AA is 500 μM . In contrast, with 2.0 mM NADH assistance (NADH was employed to reduce Au (III) into Au (I) at first, and then Au (I) was reduce by AA to mediate AuNBPs growth), the system has a colorless blank and presents obvious pink color when AA concentration is 23 μM , i.e. the visual detection limit of AA is 23 μM (Figure 1-A). When AA concentration increased from 0 to 277 μM , the solution exhibited ten distinct colors from colorless to wine red, accompanied with the red-shift of the longitudinal LSPR wavelength of AuNBPs (Figure 1-A). Above results demonstrated that AuNBPs growth can be more sensitively mediated by AA with NADH assistance, and therefore the NADH-assisted AA-mediated AuNBPs growth can greatly improve the sensitivity of AuNBPs-based colorimetric assays.

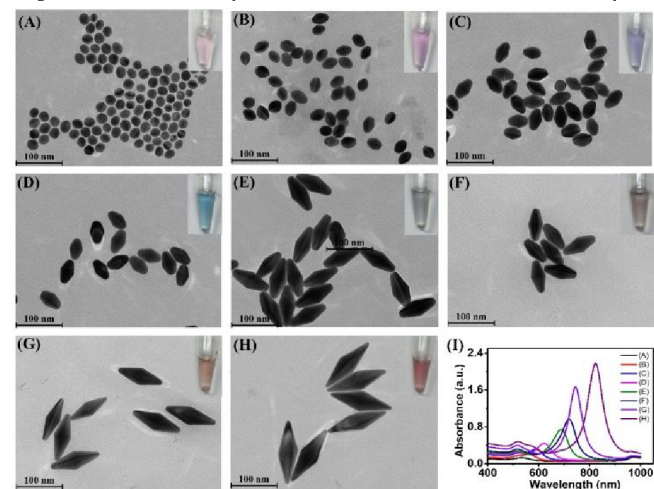


Figure 2. TEM images and photographs of the AuNBPs (A-H) obtained with different AA concentrations under the assistance of 2.0 mM NADH, and their corresponding UV-visible spectra (I). AA concentration is 25 μM (A), 55 μM (B), 70 μM (C), 90 μM (D), 105 μM (E), 115 μM (F), 160 μM (G) and 230 μM (H).

The transmission electron microscopy (TEM) images showed the morphology of Au nanoparticle regulated by AA with NADH assistance (Figure 2). With the increasing of AA concentration, the size of formed nanoparticle gradually increased, and the morphology of nanoparticles changed from spheroid structures to rice-like structures, truncated AuNBPs structures and bicuspid AuNBPs structures step by step (Figure 2). The Au nanoparticle regulated by only AA without

NADH assistance showed the similar morphology variation (Figure S1 in supporting information, SI). Compared Figure 2 with Figure S1, it can be observed that Au nanoparticles obtained with above two methods both have high monodispersity and high uniformity, which made the solution showed clearer multiple colors and thus can be more accurately and sensitively inspected by bare eye observation.

Optimization of the Conditions of NADH-assisted AA-mediated AuNBPs Growth. As we mentioned above, NADH was used to previously reduce Au (III) into Au (I) to suppress blank and improve the sensitivity of AA-mediated AuNBPs growth. Therefore, it is necessary to control ambient conditions to make NADH rapidly reduce Au (III) into Au (I) and to impede NADH further reduce Au (I) into Au (0) since the standard redox potential of NAD^+/NADH (-0.315 V vs NHE) is lower than that of dehydroascorbic acid/AA (+0.33 V vs NHE).^{26, 27} Our experiments demonstrated that the presence of CTAB and HCl can effectively impede NADH to further reduce Au (I) into Au (0). As Figure S2 (see SI) showed, when CTAB concentration was higher than 20 mM (in the presence of 25 mM HCl) or 90 mM (in the absence of HCl), the solution showed colorless, indicating that NADH can only reduce Au (III) into Au (I) and no Au (I) was reduced into Au (0) to form AuNBPs, just like previous literatures.²⁸⁻³⁰ Therefore, 118 mM CTAB and 25 mM HCl were added into our AuNBPs growth solution to impede NADH to further reduce Au (I).

The Figure S3 results (see SI) also confirmed that in the presence of 118 mM CTAB and 25 mM HCl, NADH can not further reduce Au (I) into Au (0) to promote AuNBPs growth. It was observed that in our NADH-assisted AA-mediated AuNBPs growth system, the variation of NADH concentration (from 1.5 to 2.5 mM) do not affect the maximum absorption wavelength of generated AuNBPs, whereas, the variation of AA concentration (from 0.4 to 0.5 mM) obviously lengthen the maximum absorption wavelength of generated AuNBPs (Figure S3 in SI), indicating that only AA can reduce Au (I) into Au (0) to generate AuNBPs growth in our NADH-assisted AA-mediated AuNBPs growth system.

Optimization of the ALP Enzymolysis Conditions. As we mentioned above, ALP was used as a readout enzyme to hydrolyze AAP to generate AA, and the generated AA was used to reduce Au (I) into Au (0) to mediate AuNBPs growth in this study. Thus, the pH and the concentration of Tris-HCl buffer, the DEA concentration and the AAP concentration in the ALP enzymolysis experiment were optimized. The pH of system not only affects the activity of ALP but also affects the stability of AA, and thus affects the growth of AuNBPs and finally affects the sensitivity of method. Since the AuNBPs growth is pH-sensitive,³¹ the pH of Tris-HCl buffer was optimized by directly detecting the generated AA with high performance liquid chromatography (HPLC) (details see 1.0 section and Figure S4 in SI). As showed in Figure S5-A (see SI), the peak area of AA increased with the increasing of the pH when the pH is lower than 9.0, and then the peak area of AA turn to decreased when the pH is higher than 9.5. This should be attributed that the ALP activity increased with the increasing of the pH when the pH is lower than 9.0, and too high pH (>9.5) will lead to the hydrolysis of AA. Thus, the pH of ALP enzymolysis should be controlled in the range pH 9.0 - pH 9.5, and the Tris-HCl buffer with pH 9.5 was used in our study. The concentration of tris-HCl buffer, the DEA

concentration and the AAP concentration were also optimized with the same manner, and the same trends as the pH were observed (Figure S5 B-D in SI). As Figure S5 B-D showed, the concentration of tris-HCl buffer, DEA and AAP should be controlled in the range of 25-35 mM, 20-40 mM and 65-80 mM respectively to ensure the method has high enough sensitivity and stability. Finally, 30 mM of Tris-HCl buffer (pH 9.5), 30 mM of EDA and 70 mM of AAP were used in our experiments as the optimal conditions.

Optimization of the AuNBPs Growth Solution in Multicolor Visual Detection of HER2 ECD. Under above optimal NADH-assisted AA-mediated AuNBPs growth and ALP enzymolysis conditions, the HCl and the streptavidin-linked ALP concentrations in growth solution and the incubation time of ALP were also optimized in detail to obtain high sensitivity and stability for the visual detection of HER2 ECD. The HCl in growth solution will affect the anisotropy of AuNBPs growth, and was optimized in the range of 10 to 40 mM. As Figure S6 (see SI) showed, the generated AuNBPs showed the maximum absorption wavelength (λ_{max}) of LSPR when HCl concentration was in the range of 20-30 mM. When HCl concentration decreased to 15 mM or increased to 40 mM, the sensitivity of the method dropped sharply by 36% and 48%, respectively. Hence, 25 mM was selected as optimal HCl concentration. In the detection of HER2 ECD, the streptavidin-linked ALP amount binding on the surface of microplate directly affect the sensitivity of the immunosensor, and thus streptavidin-linked ALP concentration was optimized in the range of 5 to 40 nM. The maximum absorption wavelength of LSPR increased with the increasing of concentration from 5 to 20 nM and then decreased with the increasing of concentration from 20 to 40 nM (Figure S6-B in SI). When ALP concentration varied in the range of 15-25 mM, the sensitivity of the method changed within 10%. Hence, 20 nM was selected as optimal streptavidin-linked ALP concentration. The incubation time of streptavidin-linked ALP was optimized from 15 to 90 min. The maximum absorption wavelength of LSPR increased when the incubation time was less than 60 min, and then reached a platform when the incubation time was over 60 min (Figure S6-C in SI). Hence, 60 min was chosen as the optimum incubation time.

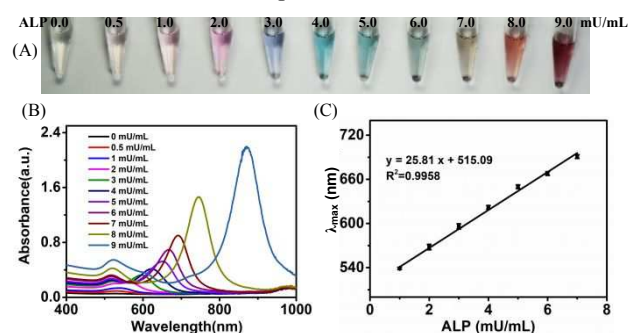


Figure 3. The photographs (A) and UV-visible spectra (B) of AuNBPs solution obtained with NADH-assisted AA-mediated under different ALP concentrations, and the linear relationship between maximum absorption wavelength (λ_{max}) and ALP concentration (C).

Detection of ALP. Under the optimal ALP enzymolysis conditions, when the ALP concentration increased from 0 to 9 mU/mL, the AuNBPs solution showed a vivid color change with a red-shift of longitudinal LSPR wavelength of AuNBPs

from 520 to 871 nm (Figure 3A-B). The color change can be clearly observed by bare eye when ALP concentration is 1.0 mU/mL, i.e. the visual detection limit is 1.0 mU/mL for ALP. The max absorption wavelength (λ_{\max}) exhibited a good linear relationship with ALP concentration from 1 to 7 mU/mL (Figure 3-C), and 0.25 mU/mL of ALP resulted in an obvious absorption of LSPR after deducting blank and noise. Thus, the UV-visible spectrophotometry detection limit, which was defined as the lowest concentration that can be detected by spectrophotometry, was 0.25 mU/mL for ALP. Compared to the other colorimetric methods, the proposed method showed more colors, and had similar or better detection sensitivity for ALP.^{24, 32, 33}

Multicolor Visual Detection of HER2 ECD. As shown in Figure 4A, when the HER2 ECD concentration increased from 0 to 9 ng/mL, the solution color changed from colorless to pink, purple, bluish violet, blue, green, olive, brown, grayed and wine red. Correspondingly, the maximum absorption wavelength (λ_{\max}) of solution shifted from 526 to 814 nm (Figure 4-B). The color change can be clearly confirmed with bare eye when HER2 ECD concentration is 0.5 ng/mL, i.e. the visual detection limit of our immunosensor is 0.5 ng/mL for HER2 ECD. The maximum absorption wavelength (λ_{\max}) had a good linear correlation with the HER2 ECD concentration in the range of 1.0 - 7.0 ng/mL (Figure 4-C). As Figure S7 (see SI) showed, 0.05 ng/mL of HER2 ECD resulted in an obvious absorption of LSPR after deducting blank and noise, i.e. the UV-visible spectrophotometry detection limit, which was defined as the lowest concentration that can be detected by spectrophotometry, was 0.05 ng/mL for HER2 ECD. It was reported that as a breast cancer biomarker, the HER2 ECD levels in serum can be used as an index for diagnosing breast cancer with a cut-off value of 15 ng/mL.^{3, 4} The visual detection limit of our immunosensor for HER2 ECD is much lower than the cut-off value, indicating that our immunosensor can be used as promising alternative for the rapid early diagnosis of breast cancer. Compared to the other HER2 ECD detection method including ELISA,^{8, 34-40} the proposed assay not only has a significantly lower detection limit but also exhibited multiple colors (Table S1 in SI), although the proposed immunosensor still has some inherent shortcomings like ELISA, such as requirements of complicated operation and temperature control instrument, which impeded its application in the home. Moreover, compared to the other multicolor assays, our method exhibited more colors in a narrower range of target concentration, which makes it more suitable for the visual detection of the biological target with cut-off value or normal reference range.

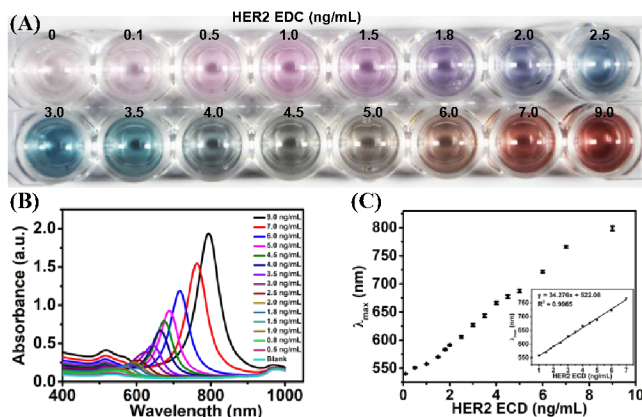


Figure 4. The photographs (A) and UV-visible spectra (B) of AuNBPs solution when the proposed immunosensor was used to detect HER2 ECD, and the linear relationship between maximum absorption wavelength (λ_{\max}) and HER2 ECD concentration (C).

To evaluate the selectivity of the proposed multicolor immunosensor, IgG (immunoglobulin G), BSA (bull serum albumin), and CEA (carcino-embryonic antigen) were selected as interferences. Under the optimum conditions, the HER2 ECD (3 ng/mL) and the interferences (30 ng/mL) were tested by the proposed multicolor immunosensor. As shown in Figure 5, the interferences exhibited similar result as the blank without spectrogram of AuNBPs growth and vivid color, and only HER2 ECD sample induced AuNBPs growth with the corresponding spectrogram and showed green color. The results indicated the proposed immunosensor had high selectivity for HER2 ECD.

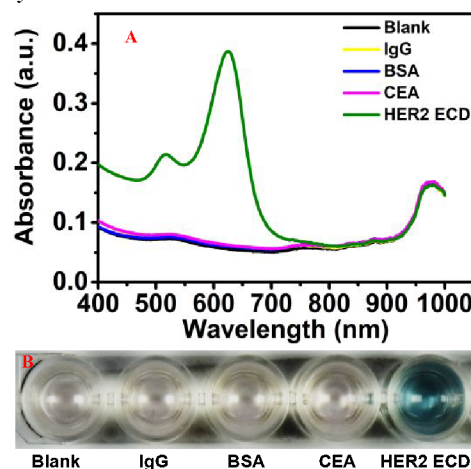


Figure 5. The UV-visible spectra (A) and photographs (B) for detecting different proteins (IgG, BAS, CEA and HER2 ECD) with the proposed multicolor immunosensor under optimal conditions. The HER2 ECD concentration was 3 ng/mL, and the concentration of other proteins was all 30 ng/mL.






Detection of Serum Samples. In order to evaluate the potential application of the proposed multicolor immunosensor for clinical diagnosis, the serum samples spiked with four levels of HER2 ECD were detected. As results shown in Table 1, the serum samples spiked with different HER2 ECD concentrations (5.5, 8.5, 13.5, and 15.5 ng/mL) displayed corresponding different colors. The UV-visible spectrometry has a relative standard deviation (RSD, $n=5$) < 5% and a recovery of 94% - 96%. The results obtained with our immunosensor were consistent with those obtained with ELISA, verifying that the proposed immunosensor is reliable and can be applied to the visual detection of HER2 ECD in the early diagnosis and/or combination therapy of HER2-dependent breast cancers. In addition, the proposed immunosensor has distinguishable color change between 13.5 ng/mL and 15.5 ng/mL of HER2 ECD concentration, which was helpful to judge if the HER2 ECD concentration in serum exceeds the cut-off value (15 ng/mL) by bare eye observation.

CONCLUSIONS

In summary, we herein developed a method for sensitively mediating AuNBPs growth with AA under NADH assistance, and further fabricated a high-resolution multicolor immunosensor for sensitive visual detection of HER2 ECD, a

breast cancer biomarker, by using AuNBPs as signal and antibody as recognition probe. The NADH-assisted AA-mediated method effectively suppress blank and greatly improve sensitivity of AA-mediated AuNBPs growth, which makes us can use low concentration of AA to mediate AuNBPs growth to generate more colorful and clearer color changes. The proposed multicolor immunosensor has a high resolution and more color changes corresponding to HER2 ECD concentrations. It can be used to detect as little as 0.5 ng/mL of HER2 ECD concentration by bare eye observation and 0.05 ng/mL of HER2 ECD concentration by UV-visible spectrophotometry. With help of the multicolor immunosensor, we have successfully detected HER2 ECD in human serum with a recovery of 94%-96% and an RSD ($n = 5$) $< 5\%$, and the results obtained with our immunosensor were consistent with those obtained with ELISA. The proposed immunosensor exhibited a vivid multicolor change, has low visual detection limit, excellent specificity and reproducibility, and robust resistance to matrix. Especially, the visual detection limit of our immunosensor is much lower than the cut-off value (15 ng/mL) of HER2 ECD in serum, which was used as breast cancer index. All above features makes our immunosensor a promising assay for the early diagnosis of HER2-dependent breast cancers in clinical diagnosis. It must be mentioned that our immunosensor may be expended as a general method for the visual detection of other cancer biomarker by using the corresponding antibody as recognition probe.

Table 1: Analytical results of HER2 ECD in serum samples

Sample	HER2 ECD added (ng/mL)	Bare eye observation	HER2 ECD detected			Ab100510-HER2 EDC ELISA Kit (ng/mL)
			UV-visible spectrometry			
			Concentration (ng/mL)	RSD (n=5)	Recovery	
1	0.0		~0.5	5	-	0.48
2	5.5		5.64	4	94	5.78
3	8.5		8.61	2	96	8.89
4	13.5		13.4	3	96	13.8
5	15.5		15.2	2	95	15.6

ASSOCIATED CONTENT

Supporting Information

The Supporting Information is available free of charge on the ACS Publications website.

Details for HPLC analysis of AA, conditions optimization (Fig. S1-S7) and comparison among our method and previous methods (Table S1) (PDF).

AUTHOR INFORMATION

Corresponding Author

* E-mail: fengfu@fzu.edu.cn

Author Contributions

Prof. F.-F. Fu and Dr Z.-W. Wang perform the experimental design, data analysis and interpretation, and manuscript writing. Q. Chen, Y.-Y. Zhong, X.-H. Yu and Z.-W. Wang performed the experiments. Prof. Y.-N. Wu co-performed data analysis and interpretation. The manuscript was written through contributions of all authors, and all authors have given approval to the final version of the manuscript.

Notes

The authors declare no competing financial interest.

ACKNOWLEDGMENT

The authors gratefully acknowledge the NSFC (21976029, 21505020, 21804020), The National Key Research and Development Program of China (2017YFC1600500), Fujian Provincial Department of Science and Technology (2019Y0002), and the Program for Fujian agriculture and forestry university Outstanding Youth Scientific Research (201810) for financial support.

REFERENCES

- Ross, J. S.; Fletcher, J. A. *Am. J. Clin. Pathol.* **1999**, 112, 53-67.
- Pupa, S.; Menard, S.; Morelli, D.; Pozzi, B.; De, G. P.; Colnaghi, M. *Oncogene* **1993**, 8, 2917-2923.
- Schippinger, W.; Regitnig, P.; Bauernhofer, T.; Ploner, F.; Hofmann, G.; Krippel, P.; Wehrschütz, M.; Lax, S.; Carney, W.; Neumann, R. *Oncol. Rep.* **2004**, 11, 1331-1336.
- Pallud, C.; Guinebretiere, J.; Guepratte, S.; Hacene, K.; Neumann, R.; Carney, W.; Pichon, M. *Anticancer Res.* **2005**, 25, 1433-1440.
- Zhang, Z.; Li, C.; Fan, H.-W.; Xiang, Q.; Xu, L.; Liu, Q.-X.; Zhou, S.; Xie, Q.-F.; Chen, S.-Q.; Mu, G.-Y.; Cui, Y.-M. *Breast Cancer Res. Treat.* **2018**, 172, 513-521.
- Carney, W. P.; Bernhardt, D.; Jasani, B. *Biomarkers in Cancer* **2013**, 5, 31-39.
- Lee, J. S.; Son, B.-H.; Ahn, S. H. *J. Breast Cancer* **2012**, 15, 189-196.
- Savino, M.; Parrella, P.; Copetti, M.; Barbano, R.; Murgo, R.; Fazio, V. M.; Valori, V. M.; Carella, M.; Garrubba, M.; Santini, S. A. *Anal. Cell. Pathol.* **2009**, 31, 203-211.
- Al-Khafaji, Q.; Harris, M.; Tombelli, S.; Laschi, S.; Turner, A.; Mascini, M.; Marrazza, G. *Electroanalysis* **2012**, 24, 735-742.
- Shen, C.-C.; Zeng, K.; Luo, J.-J.; Li, X.-Q.; Yang, M.-H.; Rasooly, A. *Anal. Chem.* **2017**, 89, 10264-10269.
- Zhang, H.-T.; Cheng, X.; Richter, M.; Greene, M. I. *Nat. Med.* **2006**, 12, 473-477.
- Jo, H.; Her, J.; Ban, C. *Biosens. Bioelectron.* **2015**, 71, 129-136.
- Ha, J.-H.; Seong, M.-K.; Kim, E.-K.; Lee, J. K.; Seol, H.; Lee, J. Y.; Byeon, J.; Sohn, Y.-J.; Koh, J. S.; Park, I.-C. *J. Breast Cancer* **2014**, 17, 33-39.
- Daniel, M.-C.; Astruc, D. *Chemical reviews* **2004**, 104, 293-346.
- Alivisatos, P. *Nat. Biotechnol.* **2004**, 22, 47.
- Cao, J.; Sun, T.; Grattan, K. T. *Sensors and Actuators B: Chemical* **2014**, 195, 332-351.
- Zhang, Z.-Y.; Wang, H.; Chen, Z.-P.; Wang, X.-Y.; Choo, J.; Chen, L.-X. *Biosens. Bioelectron.* **2018**, 114, 52-65.
- Li, Y.-Y.; Ma, X.-M.; Xu, Z.-M.; Liu, M.-H.; Lin, Z.-Y.; Qiu, B.; Guo, L.-H.; Chen, G.-N. *Analyst* **2016**, 141, 2970-2976.
- Zhang, Z.-Y.; Chen, Z.-P.; Cheng, F.-B.; Zhang, Y.-W.; Chen, L.-X. *Biosens. Bioelectron.* **2017**, 89, 932-936.
- Chen, Z.-T.; Lin, Y.; Ma, X.-M.; Guo, L.-H.; Qiu, B.; Chen, G.-N.; Lin, Z.-Y. *Sensors and Actuators B: Chemical* **2017**, 252, 201-208.
- Li, Q.; Zhuo, X.-L.; Li, S.; Ruan, Q.-F.; Xu, Q.-H.; Wang, J.-F. *Adv. Opt. Mater.* **2015**, 3, 801-812.
- Kirschner, M. S.; Lethiec, C. M.; Lin, X.-M.; Schatz, G. C.; Chen, L.-X.; Schaller, R. D. *ACS photonics* **2016**, 3, 758-763.
- Lombardi, A.; Loumagne, M.; Crut, A. I.; Maioli, P.; Del Fatti, N.; Vallée, F.; Spuch-Calvar, M.; Burgin, J.; Majimel, J. r.; Tréguer-Delapierre, M. *Langmuir* **2012**, 28, 9027-9033.
- Xu, S.-H.; Ouyang, W.-J.; Xie, P.-S.; Lin, Y.; Qiu, B.; Lin, Z.-Y.; Chen, G.-N.; Guo, L.-H. *Anal. Chem.* **2017**, 89, 1617-1623.
- Sánchez-Iglesias, A.; Winkelmann, N.; Altantzis, T.; Bals, S.; Grzelczak, M.; Liz-Marzán, L. M. *J. Am. Chem. Soc.* **2016**, 139, 107-110.
- Wilson, D. F.; Erecińska, M.; Dutton, P. L. *Annu. Rev. Biophys. Bioeng.* **1974**, 3, 203-230.
- Nanni Jr, E. J.; Stallings, M. D.; Sawyer, D. T. *J. Am. Chem. Soc.* **1980**, 102, 4481-4485.
- Xiao, Y.; Shlyahovsky, B.; Popov, I.; Pavlov, V.; Willner, I. *Langmuir* **2005**, 21, 5659-5662.
- Xiao, Y.; Pavlov, V.; Levine, S.; Niazov, T.; Markovitch, G.; Willner, I. *Angew. Chem., Int. Ed.* **2004**, 43, 4519-4522.
- Liang, P.-P.; Yu, H.-X.; Guntupalli, B.; Xiao, Y. *ACS Appl. Mater. Interfaces* **2015**, 7, 15023-15030.
- Qi, Y.; Zhu, J.; Li, J.-J.; Zhao, J.-W. *J. Nanopart. Res.* **2016**, 18, 190.
- Gao, J.; Jia, M.-N.; Xu, Y.-Y.; Zheng, J.-M.; Shao, N.; Zhao, M.-P. *Talanta* **2018**, 189, 129-136.
- Zhang, Z.-Y.; Chen, Z.-P.; Wang, S.-S.; Cheng, F.-B.; Chen, L.-X. *ACS Appl. Mater. Interfaces* **2015**, 7, 27639-27645.
- Niazi, J. H.; Verma, S. K.; Niazi, S.; Qureshi, A. *Analyst* **2015**, 140, 243-249.
- Marques, R. C.; Viswanathan, S.; Nouws, H. P.; Delerue-Matos, C.; González-García, M. B. *Talanta* **2014**, 129, 594-599.
- Ravalli, A.; da Rocha, C. G.; Yamanaka, H.; Marrazza, G. *Bioelectrochemistry* **2015**, 106, 268-275.
- Pacheco, J. G.; Rebelo, P.; Freitas, M.; Nouws, H. P. *Sensors and Actuators B: Chemical* **2018**, 273, 1008-1014.
- Qureshi, A.; Gurbuz, Y.; Niazi, J. H. *Sensors and Actuators B: Chemical* **2015**, 220, 1145-1151.
- Arya, S. K.; Zhuravski, P.; Jolly, P.; Batistuti, M. R.; Mulato, M.; Estrela, P. *Biosens. Bioelectron.* **2018**, 102, 106-112.
- Kim, M. I.; Ye, Y.; Woo, M. A.; Lee, J.; Park, H. G. *Adv. Healthcare Mater.* **2014**, 3, 36-41.

